



Clusters in intense FLASH pulses: ultrafast ionization dynamics and electron emission studied with spectroscopic and scattering techniques

C Bostedt, M Adolph, E Eremina, M Hoener, D Rupp, S Schorb, H Thomas,
a R B de Castro, T Möller

► To cite this version:

C Bostedt, M Adolph, E Eremina, M Hoener, D Rupp, et al.. Clusters in intense FLASH pulses: ultrafast ionization dynamics and electron emission studied with spectroscopic and scattering techniques. *Journal of Physics B: Atomic, Molecular and Optical Physics*, 2010, 43 (19), pp.194011. 10.1088/0953-4075/43/19/194011 . hal-00569845

HAL Id: hal-00569845

<https://hal.science/hal-00569845>

Submitted on 25 Feb 2011

HAL is a multi-disciplinary open access archive for the deposit and dissemination of scientific research documents, whether they are published or not. The documents may come from teaching and research institutions in France or abroad, or from public or private research centers.

L'archive ouverte pluridisciplinaire **HAL**, est destinée au dépôt et à la diffusion de documents scientifiques de niveau recherche, publiés ou non, émanant des établissements d'enseignement et de recherche français ou étrangers, des laboratoires publics ou privés.

Clusters in intense FLASH pulses: Ultrafast ionisation dynamics and electron emission studied with spectroscopic and scattering techniques

C Bostedt,^(1,i) M Adolph,⁽¹⁾ E Eremina,⁽¹⁾ M Hoener,^(1,ii) D Rupp,⁽¹⁾ S. Schorb⁽¹⁾,
H Thomas^(1,iii), A R B de Castro,⁽²⁾ and T Möller,⁽¹⁾

¹ *Institut für Optik und Atomare Physik, Technische Universität Berlin, Berlin Germany*

² *IFGW UNICAMP, Campinas SP Brazil and Brazilian Synchrotron Source LNLS,
Campinas SP Brazil*

Abstract

FLASH, the first FEL operating at short wavelength, has paved the way for novel types of experiments in many different scientific disciplines. Key questions for the first experiments with this new type of light source are linked to light – matter interaction and ionisation processes. This paper gives an overview of the ultrafast ionisation dynamics and electron emission of pure and doped rare gas clusters illuminated with intense short-wavelength pulses by summarizing the findings of recent years work at FLASH. Atomic clusters are ideal for investigating the light – matter interaction because their size can be tuned from the molecular to the bulk regime thus allowing to distinguish between intra and interatomic processes. The ionisation processes turned out to be strongly wavelength dependent. Plasma absorption, while dominant at 13 eV becomes insignificant at photon energies above 40 eV. The cluster ionisation and disintegration proceeds in several steps on a time scale from fs to ps. Insight into the involved processes can be obtained with ion and electron spectroscopy. The high intensity of FLASH pulses opens the door for a new imaging approach to study nanoparticles. Scattering patterns of single and few clusters can be recorded in a single shot. Initial results of scattering experiments and their comparison to Mie-calculations show that two and three dimensional structural information of gas phase particles can be obtained this way.

I – Introduction

Short wavelength FELs, especially FLASH [1] at DESY as the first source of this new type, have opened the door for novel types of experiments in many different disciplines, ranging from non-linear processes in atoms and molecules to ultrafast processes in condensed matter and plasma physics [2]. Experiments at FLASH have started in 2001 with a study on the ultrafast ionisation dynamics of clusters [3]. A key question for the first experiments with intense short-wavelength pulses concerns light matter interaction. Understanding the interaction of light with matter has been a central theme of physics over the past century, starting with the concept of the photon and the inception of quantum theory. The continuing advance in laser technology has made it possible to explore regimes of non-linear light – matter interaction. With free electron laser type sources such as FLASH, we are now witnessing the discovery of new light induced processes in the soft x-ray regime.

One of the most exciting prospects of research with x-ray lasers is direct imaging of nonperiodic nanoscale objects, such as large molecules, nanocrystals, biomolecules, living cells and viruses. Understanding the interaction of intense x-ray pulses with atomic and molecular systems and the underlying physical processes is crucial for the success of these imaging experiments. For the experimental investigation of matter in intense light pulses atomic clusters are ideal because their size can be tuned from the molecular to the bulk regime and there is no energy dissipation into the surrounding media. As we will see, the ionisation dynamics of clusters in intense laser pulses depends considerably on the radiation wavelength. Work with intense infrared (IR) lasers has been started in the nineties (see for example [4]). In the IR spectral regime, a transient nanoplasma is created (*inner ionisation*) [5] which is then efficiently heated by inverse Bremsstrahlung (IBS) and resonant plasmon excitations leading to removal of the electrons (*outer ionisation*) [6, 7], finally resulting in Coulomb explosion of the cluster. Because heating by IBS scales with $\lambda^{8/3}$ [8, 9], it was a big surprise when the first experiments at FLASH at 100 nm wavelength reported unexpectedly high energy absorption and a complete Coulomb explosion at a power density of 10^{13} W/cm² [3]. Shortly after the first experiments it became possible to extend the studies to shorter wavelength [10] and ultimately allowing ionisation of inner shell electrons [11, 12]. The present research on clusters in intense FEL beams focuses on the following issues:

- What are the dominant ionisation processes?
- Which atomic charge states are formed *inside* highly charged clusters?

- How does the removal of innershell electrons affect the electron dynamics and photo absorption?
- What is the effect of secondary electrons, e.g. Auger electrons?
- How does the chemical composition affect the ultrafast dynamics (non-metal/metal)?
- What is the time scale of electron removal (valence/innershell) from the cluster atoms?
- Finally, can Coulomb explosion be delayed by a tamper?

The last two points are especially interesting in view of the imaging of nanoparticles. Generation of unbound electrons inside the cluster results in the reduction of the contrast and thus hinders imaging.

This paper gives an overview of the achievements at FLASH during the first years of operation. After an experimental section, the results of ion and electron dynamics in highly excited clusters obtained with spectroscopic techniques are reviewed. Finally first results of single shot scattering experiments with single clusters are presented.

II – Experimental

The experiments are performed at the FLASH free electron laser in Hamburg [1] at photon energies between 13 and 90.5 eV. In the single bunch operation mode FLASH typically delivers average pulse energies of 50 μJ and pulse durations of about 20 fs [13]. The photon beam is focused either with the ellipsoidal beamline mirror under grazing incidence down to a spot size of 20 μm full width at half maximum (FWHM) [14] or with a multilayer mirror to a focal spot of 5 – 10 μm FWHM resulting in peak intensities up to a few $10^{15}\text{W}/\text{cm}^2$.

The clusters are produced by expanding pure or mixed rare gases through a cryogenically cooled, pulsed nozzle, either with a diameter of the opening cone of 100 micron (half opening angle 15 degree) or with 200 micron diameter and 4 degree half opening cone angle. The cluster beam is heavily diluted with a double skimmer setup to avoid space charge effects in the interaction region. For the spectroscopy experiments, the average cluster size is derived from scaling laws [15, 16]. For some experiments Xe core – Ar shell clusters are prepared. In this case their size and composition are derived from empirical laws obtained in early work on mixed clusters [11, 17-19]. For the imaging experiments very large clusters are prepared by expanding a gas mixture of 5% Xe in Ar at 120 K and up to 5 bar total pressure. Under these conditions the Xe partial pressure is several times higher than the vapour pressure at 120 K and to the best of our knowledge scaling laws do not exist for these extreme expansion conditions. To pick single

clusters an additional piezo driven slit assembly is mounted directly in front of the interaction region which was tuned so that on average less than one cluster is in the focal volume.

For electron and ion detection time-of-flight (tof) type spectrometers are used. For ion detection the tof is usually operated with 1.5 kV acceleration voltage. The electron spectrometer is field free and mounted perpendicular to the laser polarization plane to increase the signal contrast between the atom and cluster contributions [10]. Due to the apertures in the spectrometer the electron detection is limited to a few percent of the full solid angle.

For the investigation of x-ray scattering from single nanoclusters we have developed a high repetition rate scattering detector (see figure 1) for use at short wavelength Free Electron Laser sources. It is based on a multi channel plate (MCP) in combination with a phosphorous screen as photon amplifier and out of vacuum CCD camera. The MCP front is pulsed active with a negative voltage for only 50 ns during the arrival of the light pulse. This way photoelectrons generated by the laser pulse are deflected from the detector and the MCP is switched off prior to the arrival of ionic fragments from the nanoclusters explosion, resulting in clean scatter photon detection. The x-ray pulse can exit through a 3 mm hole in the detector assembly. This setup allows the detection of scattering angles from $\pm 3^\circ - 50^\circ$ degrees over 2π covering a large solid angle. The experiments were performed with intense soft x-ray pulses at $\lambda=13.7$ nm and pulse length of 10 – 20 fs resulting in power densities up to $5 \cdot 10^{13} \text{ W/cm}^2$. All data is stored shot by shot with a unique pulse identifier so that it can be correlated to the laser parameters in the post analysis.

III – Results

III.1 Ionisation, light absorption and fragmentation studied with ion spectroscopy

In the first study [3] on gas phase targets at FLASH Xe atoms and clusters were irradiated with intense pulses at 13 eV with a power density up to 10^{13} W/cm^2 . The energy of one photon was larger than the ionisation potential of Xe atoms and as a result cluster ionisation with a single photon became possible, in contrast to earlier work with intense IR and optical light pulses. The power density of the first FLASH experiments was sufficient to saturate the single photon absorption. Figure 2 shows a comparison of time of flight mass spectra of Xe atoms and clusters recorded at $8 \cdot 10^{12} \text{ W/cm}^2$. For the largest cluster several broad peaks can be seen which are due to singly and multiply charged Xe atoms. The most striking result is the different ion signal from atomic and cluster beams [3]. While only singly charged ions are observed after irradiation of atoms, ions with charges up to 8^+ are detected if clusters are irradiated. Doubly charged ions

resulting from ionisation of isolated Xe atoms are not detected, at least under these conditions. Clusters absorb many photons and completely disintegrate into singly and multiply charged ions. Larger cluster fragments could not be detected. The mass peaks are very broad, indicating that the ions carry high kinetic energy. This can be understood in terms of a Coulomb explosion process. The population of different ion states and their kinetic energies strongly depends on the power density [3]. This strong dependence on the power density is a clear sign that optical non-linear processes dominate the ionisation of the clusters at the power levels used. Similar results were found for Ar clusters [20]. If the power density is increased from $1 \cdot 10^{11} \text{ W/cm}^2$ to $2 \cdot 10^{13} \text{ W/cm}^2$ the mean charge state increases from 1 to ~ 3 . At the time the experiment was performed the strong absorption Xe clusters (the absorption *per atom* in the cluster), especially in comparison with isolated Xe atoms came as a surprise. In contrast to work in the IR spectral range, the effect of the radiation *field* on the cluster is expected to be small. The ponderomotive energy, which is essentially the average kinetic energy of an electron oscillating in the presence of the intense light field, is in the meV regime since it scales with $\lambda^{8/3}$. For comparison, under standard high field conditions in the IR regime it is typically 10 – 100 eV exceeding the ionisation potential of the cluster atoms. Shortly after publication of the experimental results several theoretical models have been proposed to explain the efficient absorption in clusters [21-25]. In essence, under the special conditions of this experiment with photon energies just above the ionisation potential a nanoplasma is formed which becomes temporarily strongly coupled. The efficient heating is due to inverse bremsstrahlung, however, the absorption and ionisation processes differ from that in IR-laser produced plasmas and involves complicated many body dynamics. Formation of Xe^{2+} by single photon absorption becomes possible in the plasma through barrier suppression which is prohibited in the isolated atom at this energy. Then, the plasma undergoes inverse bremsstrahlung heating. High charge states are formed through collisional ionisation and recombination of free electrons into excited states which undergo subsequent reionisation. The cluster becomes charged as energetic electrons evaporate from its surface (*outer* ionisation). During this process the cluster potential gets very steep. Finally, the cluster expands due to the pressure of the electron gas and the cluster's own charge (Coulomb explosion). This process is illustrated in figure 3. The theoretical descriptions are summarized in recent papers [7, 25, 26].

Subsequent experiments at shorter wavelength clearly above the ionisation potential made immediately clear that the role of plasma heating by inverse bremsstrahlung becomes less and less important with increasing photon energy (see also section III.2). Argon clusters irradiated with 32 nm FEL pulses and power densities of $4 \cdot 10^{14} \text{ W/cm}^2$ exhibit ion kinetic energies of a few eV only and larger cluster fragments appear [10], similar to subsequent experiments at 51 nm [27].

At shorter wavelength, when inner shell electrons can be excited, the cluster ionisation becomes strongly dependent on the photoionisation cross section. In figure 4 a comparison of ion spectra of Xe, Ar and Kr clusters irradiated by 90 eV photons is presented. At this short wavelength the main products are singly charged ions, in contrast to results in the VUV spectral range at 12.7 eV where highly charged ions are rather prominent. In an atomic beam highly charged ions are quite pronounced under the same conditions [11, 28]. This can also directly be seen in figure 4 especially for Xe where the sharp lines are due to highly charged ions from the uncondensed gas. The broad peaks are due to ions from clusters carrying kinetic energy up to a few hundred eV [12]. The intensity increases from Kr, Ar to Xe. This trend differs from the findings at lower photon energy, in particular in the IR regime. Usually Ar shows the weakest absorption and Xe the strongest, while Kr is intermediate. The trend for IR light results from the ordering of ionisation potentials and polarization. The present results at 90 eV give direct evidence that here the absorption is linked to the single photo absorption cross section at 90 eV. With 20 Mbarn Xe has by far the largest cross section which is due to excitation of 4d innershell electrons into the giant resonance peaking at 100 eV. The absorption cross section of Ar and Kr is considerably smaller, 1,5 Mbarn for Ar and 0.6 Mbarn for Kr. The cross section of Kr is rather small because 90 eV is very close to the energy of the minimum of the $4p \rightarrow d$ continuum transition matrix element (Cooper minimum) [29].

More detailed insight into the charge redistribution and cluster explosion dynamics can be obtained from heterogeneous clusters, especially core – shell systems [11]. Such systems are also relevant for future (bio-) molecule tampers in imaging experiments [30]. In first experiments, Xe atoms in the core, surrounded by an Ar shell with variable thickness are resonantly excited to high charge states. The m/q spectra for the core – shell systems are shown in figure 5. For the smaller systems ($N \approx 400$) with a thin Ar coating, the most intense signals stem from Xe fragments, namely Xe^+ , Xe^{2+} , Xe^{3+} and the Ar^+ monomer. For $m/q < 40$ (inset in figure 5) predominantly higher Ar charge states and contributions from residual gas are present. Each Ar peak consists of a sharp main line from the atomic contribution and a shoulder on each side stemming from the cluster ions which are accelerate during the Coulomb explosion in or against the direction of the detector. Xe ions with charge states higher than two, as seen in the case of atomic Xe and pure Xe clusters (compare figure 4) are not observed. The absence of highly charged Xe ions, while still the main absorption is due to Xe shows that a fast charge redistribution from the multiply charged Xe to the surrounding Ar layers takes place. The spectra of the large Xe core – Ar shell clusters ($N \approx 4000$) with a thick Ar coating of about three or more shells look completely different (figure 5, bottom). The Xe signal is only 0.6% of the total signal,

or in other words virtually absent, although the clusters contain $\sim 20\%$ Xe atoms. The dominant signal is now the Ar monomer with a significantly higher kinetic energy. Further, the multiply charged cluster Ar fragment signal becomes much more intense when compared with the smaller core – shell system (upper panel) or pristine Ar clusters (figure 4). The fact that only a very small amount of Xe^+ fragments can be detected indicates that efficient charge recombination processes take place because the fraction of Xe atoms in the cluster is much larger. Following the concept of *inner* and *outer* ionisation [5], the Xe atoms in the core become multiply ionized through the FEL pulse [28]. Therefore the strong decrease in the Xe signal and increase in Ar charge states and fragment kinetic energies for larger clusters must be caused by charge transfer, relaxation and separation dynamics, which are related to the size of the cluster and its shell structure. Considering the structure of the clusters, the detected Ar ions can only be ejected from the few outermost Ar surface layers, giving evidence of the Coulomb explosion of the cluster outer part only. The absence of the Xe signal in the m/q spectrum (figure 5, bottom) suggests that the highly charged Xe nanoplasma core recombines with quasifree electrons and thus cannot be detected. The recombination of the nanoplasma core can be understood if the details of the cluster ionisation are considered. At short wavelengths and the current power densities, the cluster ionisation is largely due to photoemission in the building Coulomb potential [10]. Since the total energy needed to remove N electrons from a cluster with N atoms scales with $N^{5/3}$, the fraction of electrons which can escape drops significantly for larger clusters. Electrons that cannot overcome the Coulomb barrier lead to the formation of the nanoplasma, akin to *inner* ionisation. These quasi-free photoelectrons thermalize and the plasma core can recombine. The nanoplasma charge imbalance is neutralized by exploding off the outermost cluster layers. Such a Coulomb explosion of the cluster outer layers and recombination of the nanoplasma core is also expected to take place in larger homogeneous clusters. However, it is much more difficult to detect because the spatial origin of the charge states cannot be tracked with conventional time of flight mass spectroscopy as in the presently investigated core – shell systems. The findings are supported by theoretical work. Efficient recombination in the cluster core has been suggested to explain differences in observed and calculated charge states [23]. Further, recent theoretical work predicts that such charge redistribution and neutralization processes will turn the cluster Coulomb explosion into a much slower ($> \text{ps}$) hydrodynamic expansion [31] [25, 32]. The presence of a neutral core inside highly ionised clusters is also supported by a recent study of Xe clusters irradiated by 90 eV photons [12]. Here, the simulation of the measured kinetic energies suggests that highly charged ions explode off the surface due to Coulomb explosion while the inner core expands in a hydrodynamic expansion. The simulation, based on a simple electrostatic model,

gave also evidence for an efficient ionisation process of the cluster in addition to the direct multistep photoemission [10] which will be described in the next section.

III.2 Electron dynamics and energy transfer process studied with electron spectroscopy

From the discussion in the preceding section it is evident, that the electron and ion dynamics of clusters exposed to intense short wavelength pulses are a highly time dependent process. During the interaction with the light pulse electrons are removed from the individual atoms (*inner* ionisation) but only the first few photoelectrons, and granted they have sufficient kinetic energy Auger electrons, can escape the cluster Coulomb potential. Ion spectroscopy can yield detailed information on the photoabsorption processes and to some extent also on the total energy absorbed. With electron spectroscopy, on the other hand, complementary information on the energy flow and deep insight into the energy exchange processes can be obtained. Photoemission gives a fingerprint of the electronic structure, in particular if applied with short wavelength radiation [33]. In the first photoemission study of clusters at FLASH Xe and Ar clusters were irradiated with 13 eV photons [34]. Here, the photon energy is only slightly larger than the Xe ionisation potential but it is still smaller than the ionisation potential of Ar. Thus, photoionisation of Ar clusters can only be accomplished by two-photon processes. Since the photon energy is just 0.8 eV larger than the ionisation of Xe, electrons emitted from atomic Xe are close to threshold forming a low energy peak below 1 eV [34]. The electron spectrum of clusters recorded at the same conditions with a power density of 5×10^{12} W/cm² exhibit also low kinetic energy with an almost thermal distribution and energies up to 30 eV. Since the ionisation potential of the cluster increases with the emission of every electron, only a few electrons can be directly emitted. On the other hand, as discussed in the preceding section, at 13 eV the clusters are efficiently heated by inverse Bremsstrahlung. The energy absorbed through the process of inverse Bremsstrahlung exceeds that due to photoionisation by more than a factor of five [26]. Therefore the electrons gain substantial energy allowing them to be evaporated from the cluster surface in a thermal process [34]. This picture is supported by recent theoretical work [35].

By going to higher photon energy the scenario changes substantially as heating by inverse Bremsstrahlung becomes insignificant [10]. For laser intensities up to 5×10^{13} W/cm² and a photon energy of 37.8 eV the cluster ionisation process is a sequence of direct electron emission events in a developing Coulomb field. A nanoplasma is formed only at the highest investigated power densities where ionisation is frustrated due to the deep cluster potential [10]. This conclusion is drawn from electron spectra presented in figure 6 and Monte Carlo simulations in figure 7. The electron spectra of Ar clusters comprising on average 80 atoms show a pronounced

peak at 22 eV and a tail to lower energies which gains intensity with increasing power density. A pronounced wing towards high kinetic energies, a characteristic for thermionic electron emission as discussed above, can not be observed. The main feature at 22 eV is due to the emission of the first photoelectron and can thus be assigned to the Ar 3p main line. The second photoelectron experiences already an increased charge in the cluster and is shifted accordingly to lower energies. At high power densities this process continuous until the electrons do not have sufficient energy to escape from the increasingly deep cluster potential and the photoionisation becomes frustrated. A quantitative description of the electron emission with Monte Carlo simulations is presented in figure 7. Here averaged spectra of individual electrons following consecutive absorption of photons are given. The broadening of the single electron spectra is due to different position of the positively charged holes in cluster. The sum spectrum exhibits a shape similar to the experimental spectra in figure 6, which also shows modelled spectra for different power densities. At the highest power density ($5 \times 10^{13} \text{ W/cm}^2$) only 20 % of the primary electrons released by photoemission from the individual cluster atoms can overcome the increasing Coulomb barrier [10]. The good agreement between experimental results and simulation and the absence of an ‘thermionic’ electron continuum, gives evidence that inverse Bremsstrahlung is insignificant at this energy (37.5 eV) and a power density up to 10^{14} W/cm^2 . Similar results have been obtained in subsequent experiments for wavelength around 60 nm [36] even though inverse Bremsstrahlung heating can in principle contribute for very long pulses at this wavelength [37].

We have already pointed out that the giant resonance of Xe which is due to 4d innershell ionisation results in a large photo absorption cross section at 90 eV. The ion spectra (figure 4) and the simulation of the kinetic energies in a simple electrostatic model [12] gave evidence, that the direct multistep photoemission cannot solely account for the large kinetic energies seen in those experiments [12]. The amount of charges on the cluster needed to model the measured ejection energies of ions is 3 – 5 times larger than the number of electrons that can leave the cluster before the multistep ionisation becomes frustrated. Here, electron spectroscopy in combination with simulations of the time dependent electron dynamics can help to identify an additional ionisation process. Figure 8 displays electron distributions of Xe clusters with a mean size of 2000 atoms for different intensities spanning a range from below $1.0 \times 10^{13} \text{ W/cm}^2$ to $5.8 \times 10^{14} \text{ W/cm}^2$. At the lowest investigated intensity of $1.0 \times 10^{13} \text{ W/cm}^2$ the photoelectron spectrum shows the pronounced peak of the 4d photoelectrons at around 22 eV and the Auger electrons around 32 eV. In addition, continua can be seen between both lines and below the 4d photo line. At the lowest intensity the photoelectron spectrum of the cluster can still be understood in the picture of the multistep model [10]. For all spectra recorded at higher intensities

an additional signal above the 4d line eV appears which increases in intensity with respect to the 4d photoline as a function of power density. It becomes most prominent at the highest power density of about $5.8 \times 10^{14} \text{ W/cm}^2$. This continuous signal stems from the 4d photoelectrons which, trapped in the strong Coulomb potential of the cluster ions, form a plasma with supra-atomic density and which undergo multiple energy-exchanging collisions in the entire cluster volume producing an electron energy distribution with a tail of fast electrons [38]. The process differs from that described in the first part of this section. At 13 eV all electrons are heated by inverse bremsstrahlung and accordingly they can overcome the Coulomb barrier in a highly charged cluster. In the case of 4d innershell ionisation with a large single photo absorption cross section, all electrons liberated from individual cluster atoms are energetically below the Coulomb barrier, once direct photoemission becomes frustrated. However, some of them can gain substantial kinetic energy by multiple energy exchanging collisions which allows them to leave the cluster [38]. Such collisional autoionisation is expected to be a general phenomenon occurring for strong atomic x-ray absorption in extended systems.

III. 3 Imaging of clusters and ultrafast processes probed with scattering techniques

One of the most fascinating prospects of research with intense short wavelength FEL pulses is imaging of single nanoparticles. The key idea is the detection of sufficient scattered photons from an object before it is destroyed in the strong light pulse [39, 40]. Here we present scattering patterns of single or a few clusters in the gas phase. The high intensity of the light pulses allows recording scattering patterns in a single shot. Details will be given in forthcoming publications [41, 42].

Figure 9 shows six single snapshots (out of thousands of similar pictures) recorded in single shots with 13 nm wavelength. The scattering patterns of single clusters (a), (c), or few clusters (b), (e) exhibit a wealth of details in contrast to featureless, smooth scattering patterns of a large ensemble of clusters (see fig 9d). These patterns, similar to diffraction patterns from a set of apertures in a flat screen, carry however 3-dim geometrical information and depend on the cluster dielectric function \mathbf{n} . As we will see they can be rather well understood in the framework of classical elastic scattering of light, e.g. *Mie scattering* [43] .

Using simple scattering models it can be concluded that, images (a) and (c) with ring patterns come from single spherical clusters of increasing sizes. Patterns (b) and (e) with stripes and fine rings come both from two clusters, but with very different geometries: (b) indicates a dumbbell geometry with the axis orthogonal to the direction of the light beam, while (e) indicates a twin

cluster, each cluster about the size of the cluster in image (d), but separated from each other by a much longer axis tilted with respect to the direction of the light beam. The pattern (d) exhibits some fine ring type structure similar to Newton rings. The “type (f)” image is due to a more complex geometry. The separation of the rings (fig. 9 (a) and (c) is inversely proportional to the cluster diameter. Obviously the total intensity of the scattering pattern increases with particle size. Under the present condition scattering pattern from clusters in the size range 20 – 300 nm radius could be recorded.

The experimental scattering patterns can be explained in the basis of scattering theory. Mie scattering refers to light scattering from homogeneous spheres with arbitrary value for the complex dielectric constant \mathbf{n} . The angular profile is obtained from a complete solution of Maxwell’s equations of electrodynamics for the electric \mathbf{E} and magnetic \mathbf{B} fields in the presence of a dielectric sphere. Further, for explaining the scattering patterns ‘*Scalar models*’ can be used [44]. They refer to light scattering from a set of pointlike independent scatterers, and apply to bodies of arbitrary shape and composition, but for them light absorption and multiple scattering are neglected. There is a rather wide range of parameters where both *Mie scattering* and *scalar models* are applicable to large Xe clusters and predict very similar angular patterns.

Figure 10 shows a more detailed comparison between a “type (b)” single shot experimental image from figure 9 and a simulation based on scalar theory for the angular distribution of light scattered by a dumbbell shaped or twin cluster with the same size. In contrast to a single spherical cluster the scattering pattern shows pronounced stripes. The stripes, as in a double slit scattering experiment, give evidence that we have two scattering centers separated by some distance. The spacing of the stripes is a measure of the particle separation d and, if the particles are in a plane parallel to the detector, it is directly proportional to $1/d$. The shape of the interference stripes in the scattering pattern yields information about the orientation of the dumbbell structure in space. In Figure 11 simulations for two clusters with identical size but different orientation with respect to the incoming photon beam are presented. It should be noted that the twinned clusters, a geometry that strongly departs from spherical, were not expected to be produced by a gas expansion cluster source. With the help of the simulated pattern in the right part of figure 10 we can conclude that the particles are 35 nm in diameter and in direct contact. Such information on clusters can not be obtained with mass spectroscopy or any spectroscopic technique. Moreover, the presence of a large number of twinned clusters in beam – of the order of one percent – produced by an adiabatic expansion of a cold gas came as quite a surprise.

The scattering pattern in figure 9 (e) which exhibits strong similarities with Newton rings can be explained in a similar way by numerical simulation [45]. In this case, the 2-dim scattering

patterns give information about the 3-dim configuration of two clusters, which are separated by a few microns. The observed Newton ring type scattering patterns results from a coherent superposition of two spherical waves. The line connecting the two clusters points into the direction of the central maximum of the Newton ring. The separation of the rings decreases with the square root of the separation from the center of the ring and it contains the information on the particle separation parallel to the FEL beam. Details will be discussed in a forthcoming publication [42]. This way 3-dim structural information can be obtained from 2-dim scattering data. Simulations similar to that shown in figure 10 (right) and figure 11 for different distances can give direct insight how the ‘stripes’ develop into ‘Newton rings’ when the angle and the separation is varied [42]. The curvature of the rings (see figure 11), and especially the asymmetry, contains information about the angle between the clusters with respect to the incoming photon beam while the spacing of the rings is a measure of their separation. Such information can also be obtained with Fourier transform techniques [40] applied to the experimental image, as pointed out very recently with a new approach [46]. Here we report on simple first results for a ‘real sample’ instead of a test object. In the present case the separation of the two clusters in figure 9 (e) of 2.8 micron is derived with the simulations [42].

With upcoming hard x-ray sources these imaging experiments offer exciting prospects such as direct imaging of clusters and other nonperiodic nanoscale objects with a resolution reaching the atomic level. Unprecedented details of cluster structure can then be revealed. The ongoing research is an important step towards this goal.

IV – Conclusion and outlook

Clusters in intense soft x-ray pulses exhibit interesting, highly time dependent ionisation dynamics. The first experiments in this field were performed with power densities up to 10^{15} W/cm². The data show that absorption and ionisation processes in the high power-density regime are strongly wavelength dependent. While at the lowest energies in the spectral range around 10 eV plasma absorption by inverse Bremsstrahlung is the dominant heating processes, it becomes less and less important with increasing photon energy. At energies above 40 eV and power densities up to 10^{13} W/cm² the cluster ionisation is best described by multistep photoionisation which becomes frustrated in the increasing Coulomb potential. This process is governed by the single photon absorption cross section and is taking place on the few fs timescale during the pulse. At the highest investigated power densities nanoplasmas with supra-atomic density are created and energy-exchanging electron collisions can lead to further cluster ionisation. The ion

spectroscopy data give evidence that although the clusters are getting highly charged, an almost neutral plasma is formed in the cluster core due to nanoplasma recombination. With scattering techniques snapshots of single clusters can be recorded with single soft x-ray light pulses. The scattering patterns provide information on the 2-dim as well as 3-dim structure of clusters and of cluster ensembles. Meanwhile time resolved experiments with pump – probe techniques have started which allow following the time evolution of cluster ionisation up to several ps. With even shorter wavelength, now already available at the LCLS, ionisation processes involving core levels can be addressed and clusters are imaged with nanometer resolution.

We would like to thank the DESY staff for their outstanding support. Funding is acknowledged from BMBF Grant No. 05KS4KTC1, DFG and HGF Virtuelles Institut VHVI- 302.

Figure Captions

Figure 1 Schematic illustration of the imaging detector for recording of scattering patterns of clusters.

Figure 2 Time-of-flight mass spectra of ionisation products of Xe atoms and clusters recorded following irradiation with 98 nm wavelength at a power density of $8 \times 10^{12} \text{ W/cm}^2$. The mean cluster size and the different charge states are indicated in the figure. The insert shows the kinetic energy of the ions as the function of the charge state. Please note that the power density was recalibrated after publication [3].

Figure 3 Schematic illustration of the ionisation of Xe clusters and subsequent Coulomb explosion. The Coulomb potential of the clusters is shown at the beginning of the FEL pulse, at its maximum and at the end of the pulse. Photons are indicated by arrows.

Figure 4 Time-of-flight mass spectra of ionisation products of Xe, Ar and Kr clusters recorded following irradiation with 13,5 nm wavelength (corresponding to 90 eV) at a power density of $4 \times 10^{14} \text{ W/cm}^2$. The mean cluster size and the different charge states are indicated in the figure.

Figure 5 m/q spectrum of Xe core–Ar shell clusters with different sizes. Top: for small clusters ($N = 400$) predominantly Xe cluster (filled) and Ar fragments are detected. Bottom: for large clusters ($N = 4000$) the Xe signal is virtually absent and the Ar signal including highly charged fragments becomes more intense. The insets depict the Xe distribution in the Ar cluster and the proposed expansion mechanism after irradiation. The arrows indicate the peak positions of high charge states [11].

Figure 6 Experimental (solid line) and modelled (dashed line) electron spectra for Ar_{80} clusters for increasing power densities from bottom to top. The numbers on the right hand side indicate how many photons fall into the absorption cross section of the cluster and how many electrons can overcome the increasing Coulomb barrier [10].

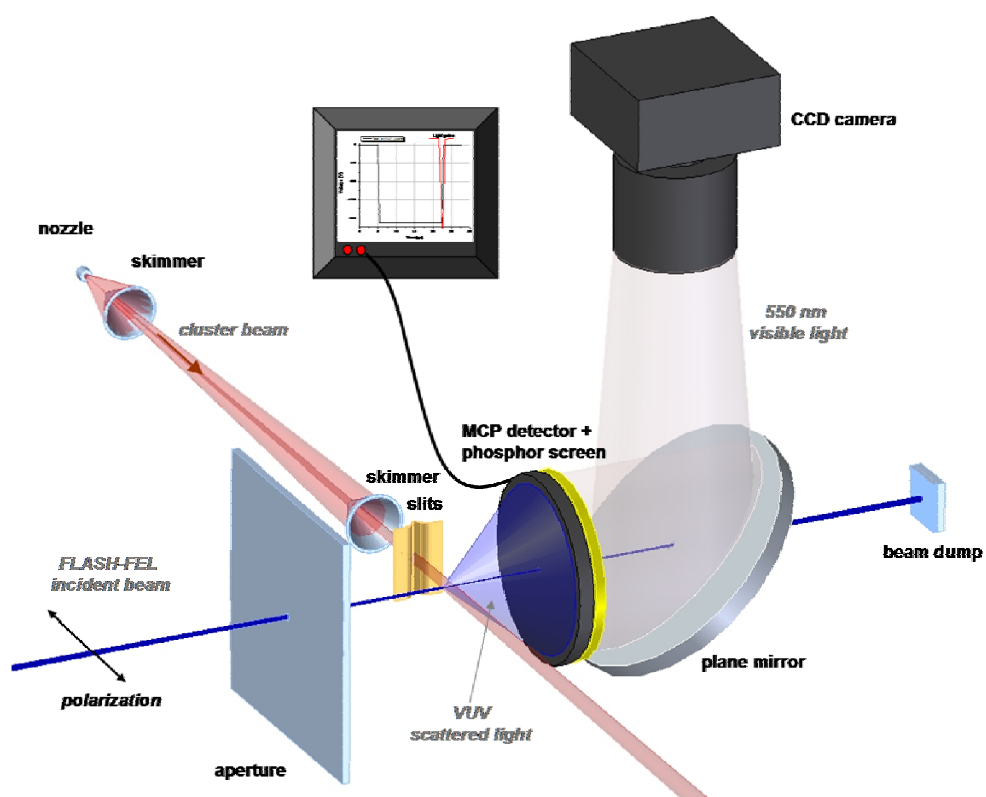
Figure 7 Monte Carlo simulations of the electron emission from an Ar_{147} cluster (see text). The averaged spectra of each emitted electron numbers (filled graphs) as well as their average (black line) are shown. For comparison with the data, the relevant broadening effects are considered [10].

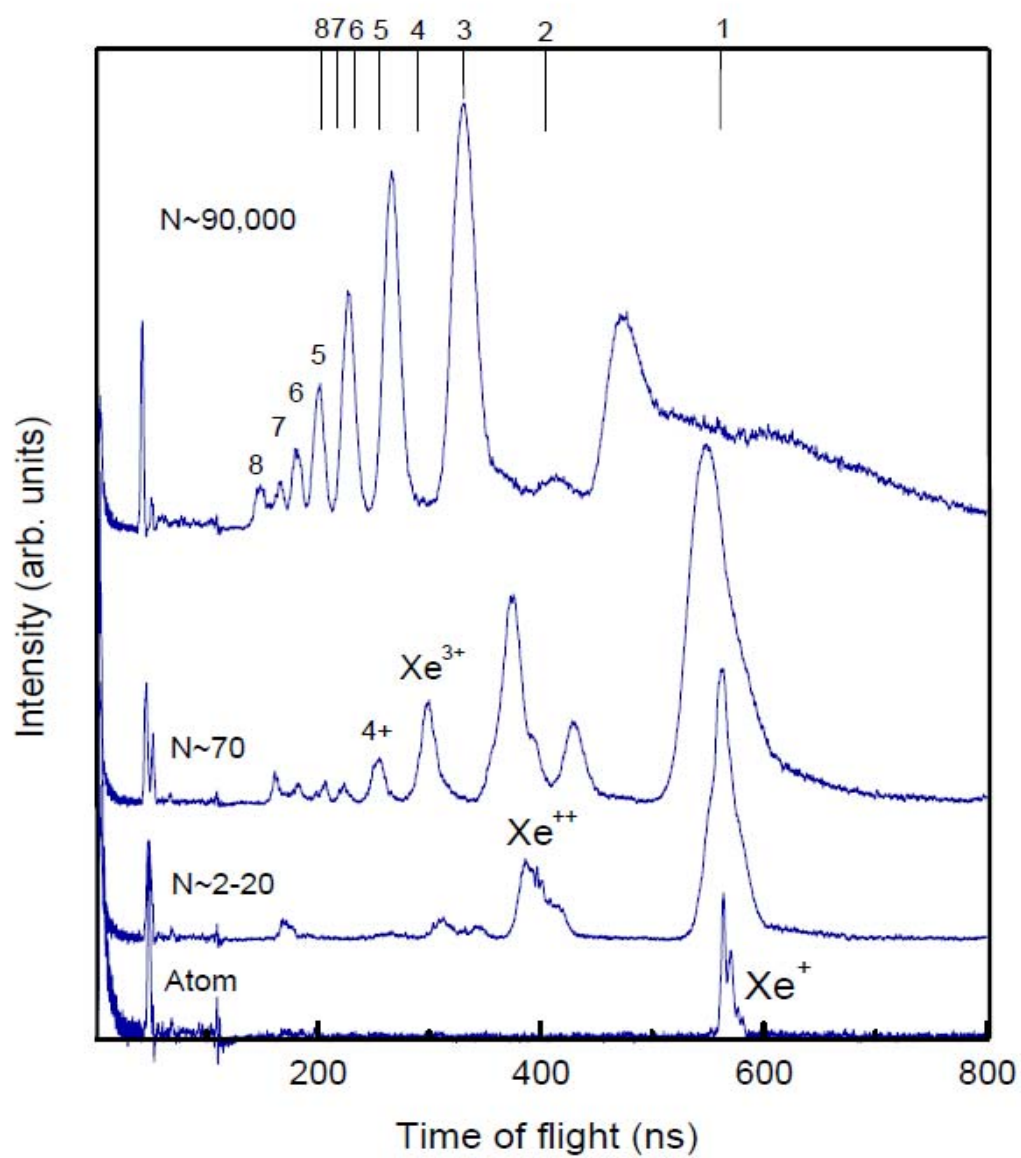
Figure 8 Electron spectra from Xe_N clusters with $N = 2000$ exposed to 10 fs FLASH pulses at 90 eV for various intensities. The line at 22 eV is due to the Xe 4d direct photoline. The shaded area marks electrons with energies higher than the photo line [38].

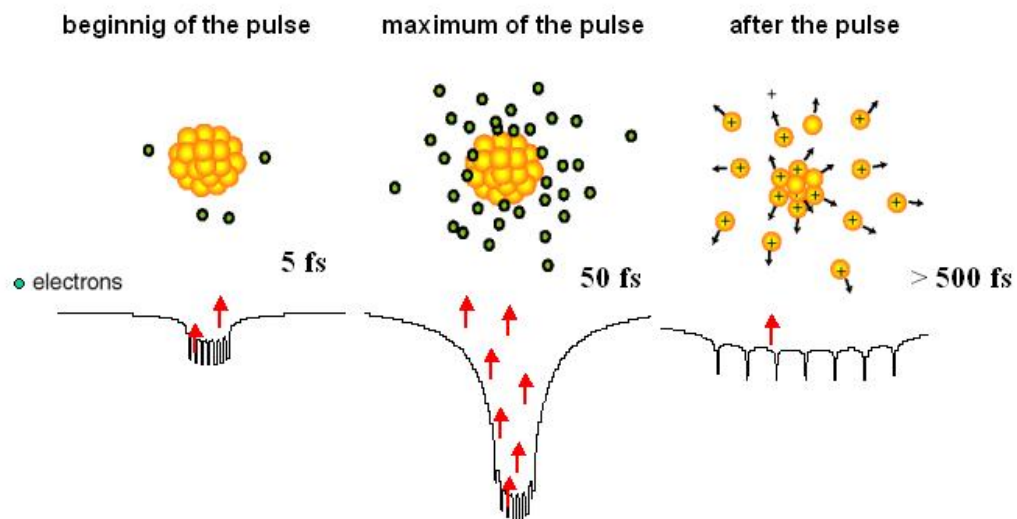
Figure 9 Single shot scattering patterns of large Xe clusters. The patterns are recorded with the detector shown in figure 1. a) a single cluster; b) two clusters in direct contact; c) a single large cluster; d) an ensemble of many clusters (more than 10) in the focus; e) two clusters separated by a large distance; f) a complex pattern from an ensemble with unknown geometry

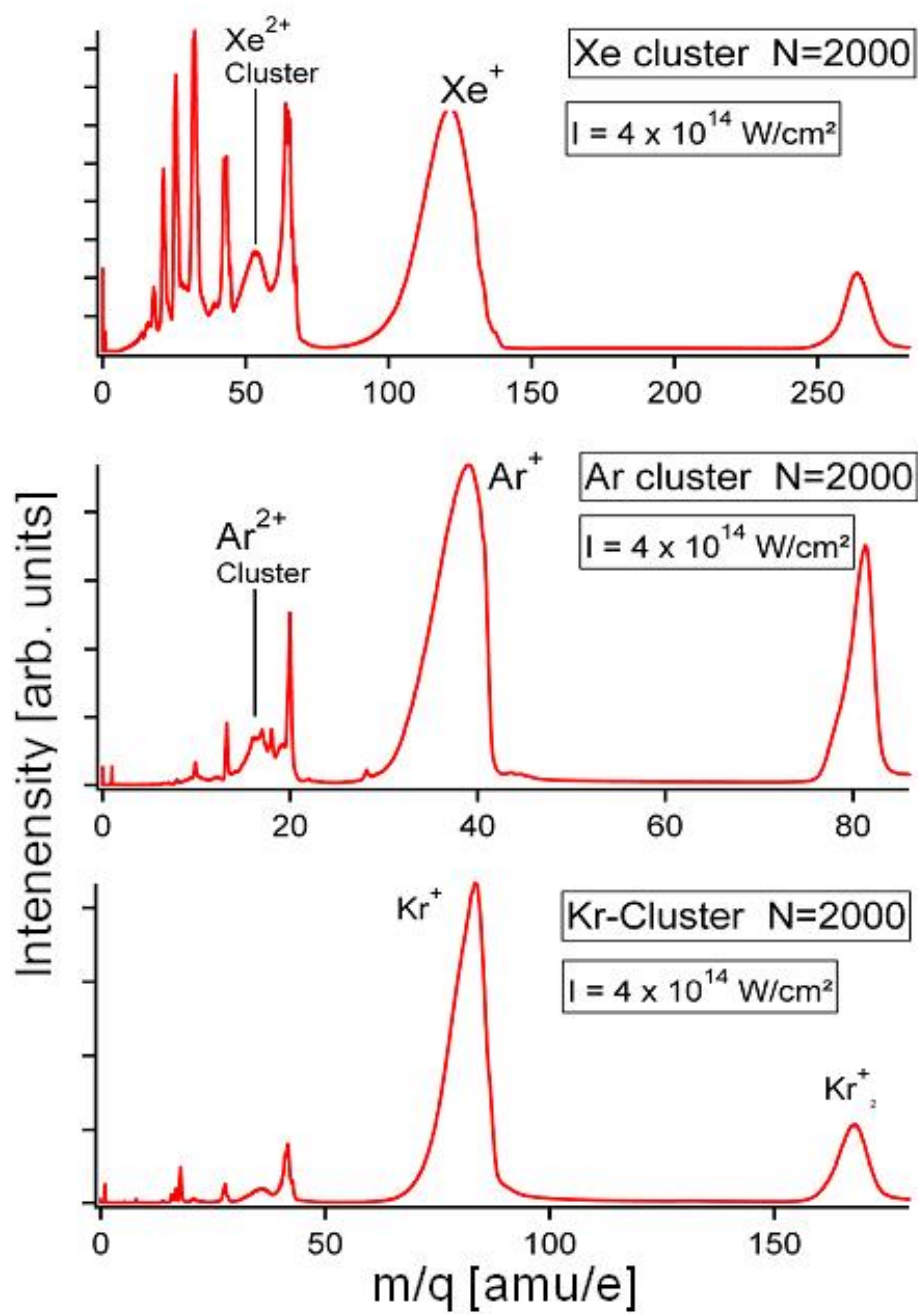
Figure 10 Detailed comparison between left: a single shot experimental image (type “b” from figure 9) and right: a simulation based on scalar theory for the angular distribution of light scattered by a dumbbell shaped or twin cluster with the same size.

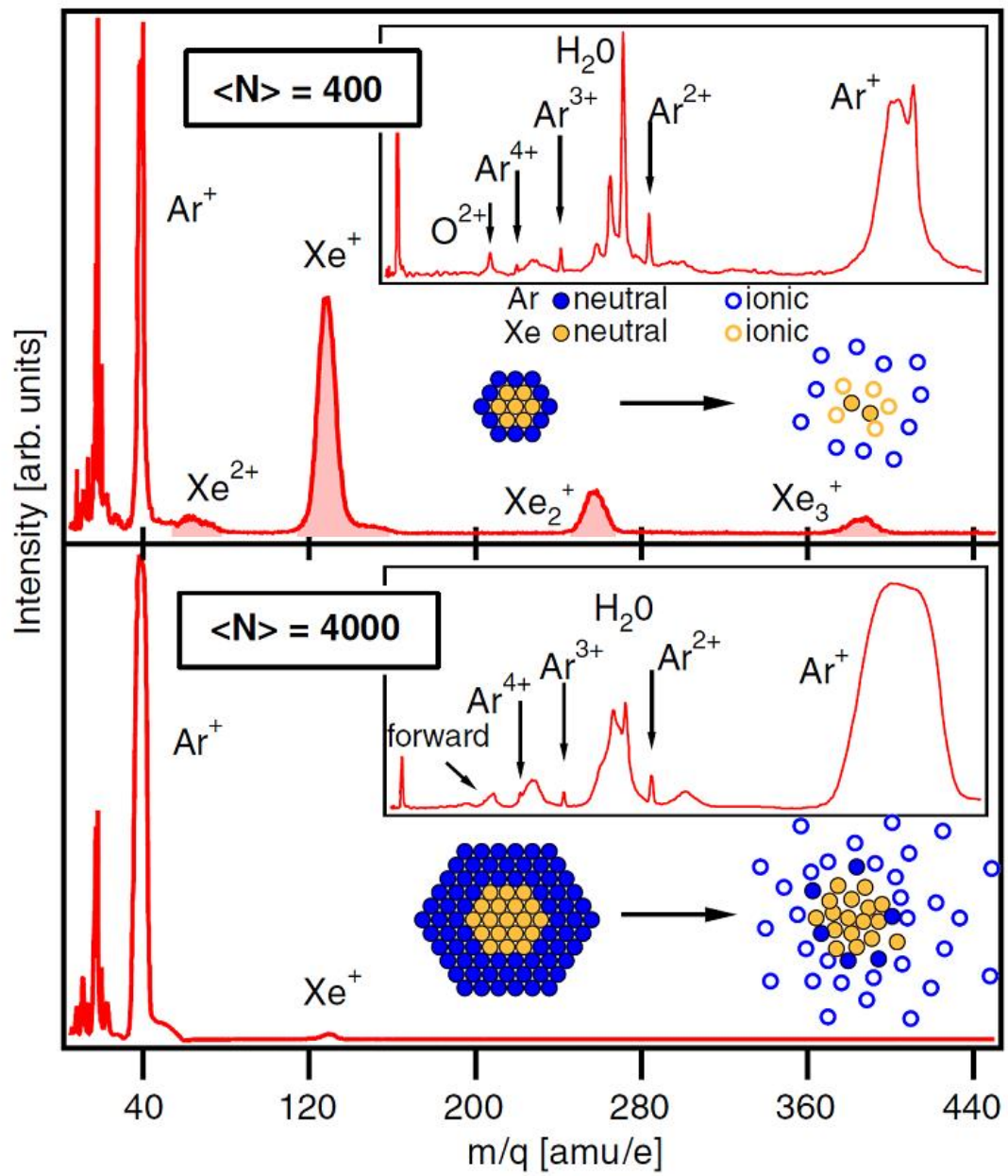
Figure 11 Simulations for two clusters with identical size but different orientation with respect to the incoming photon beam.

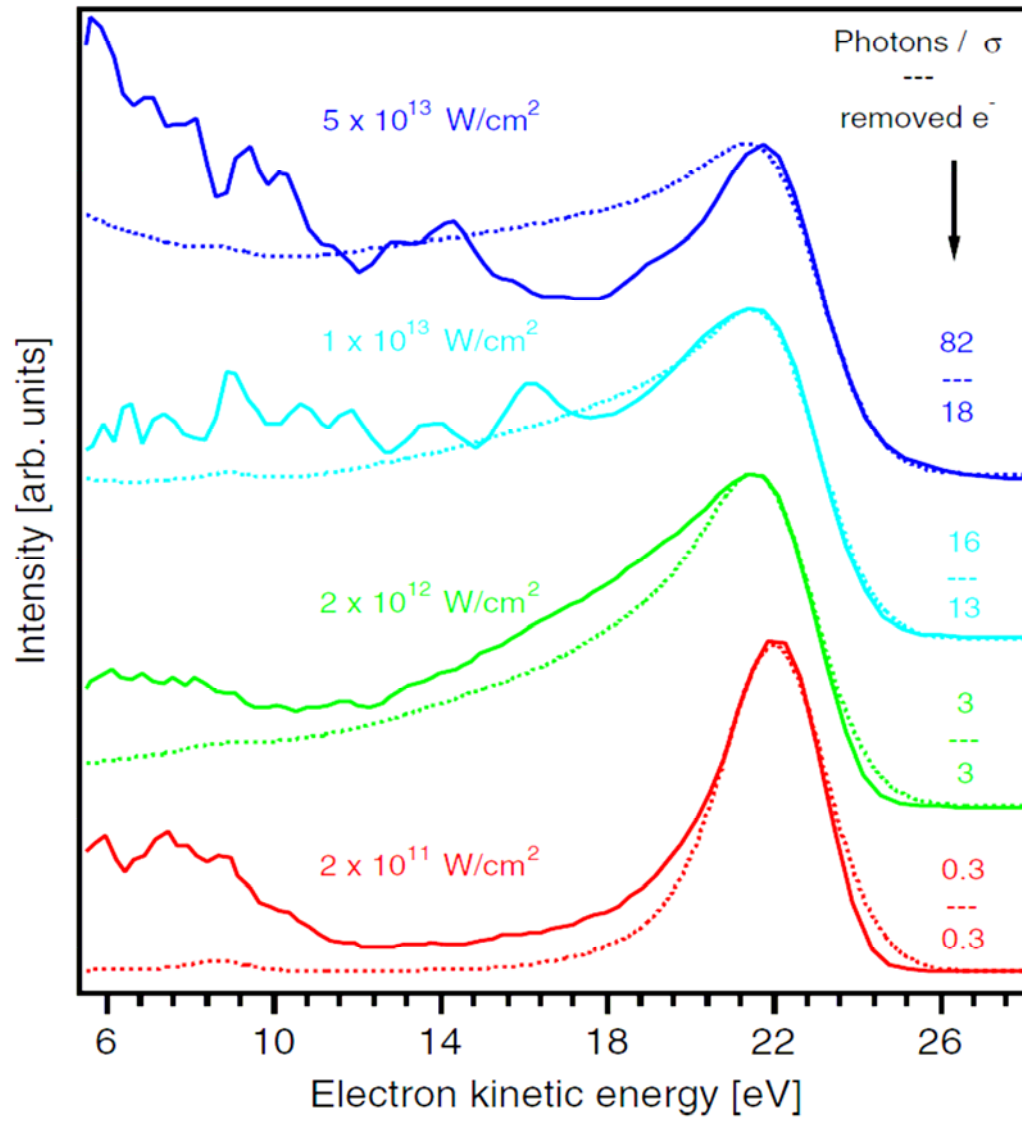


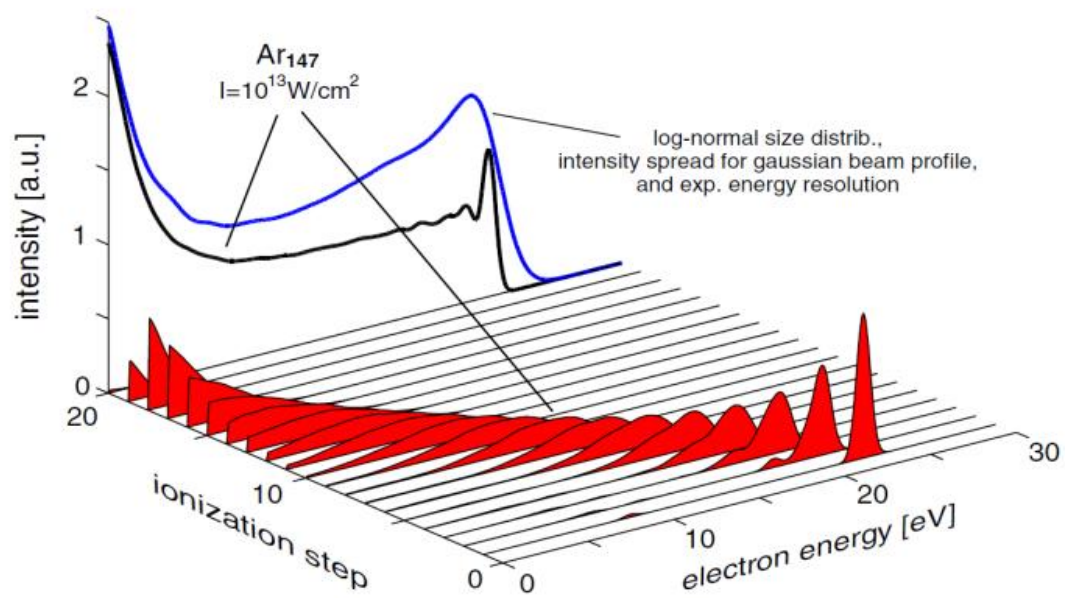


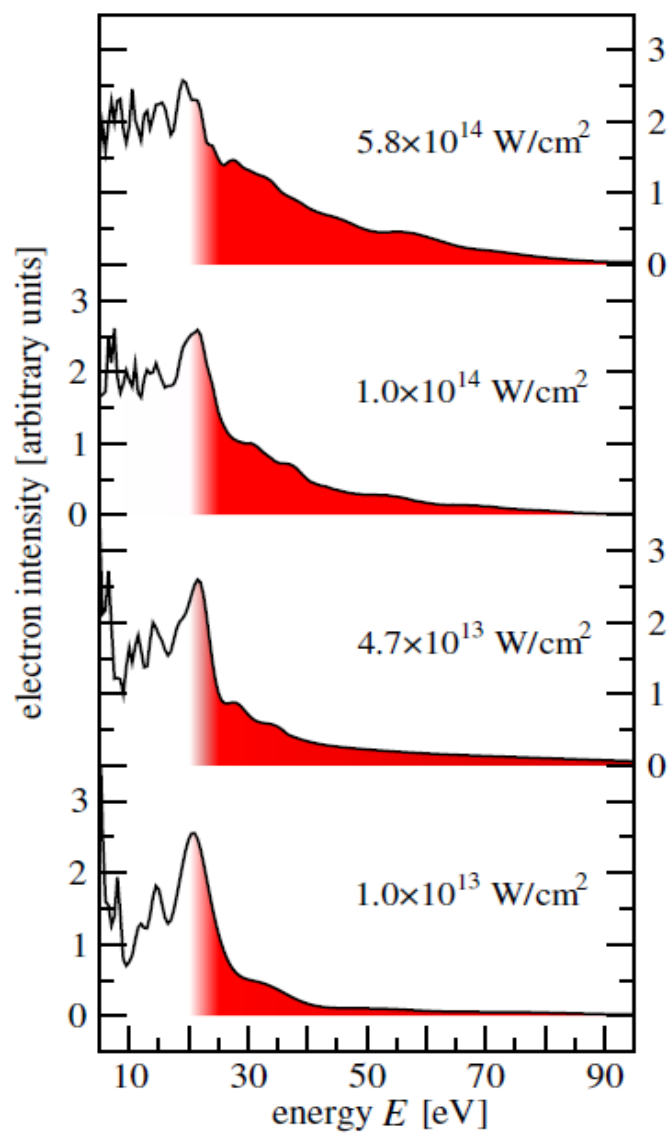


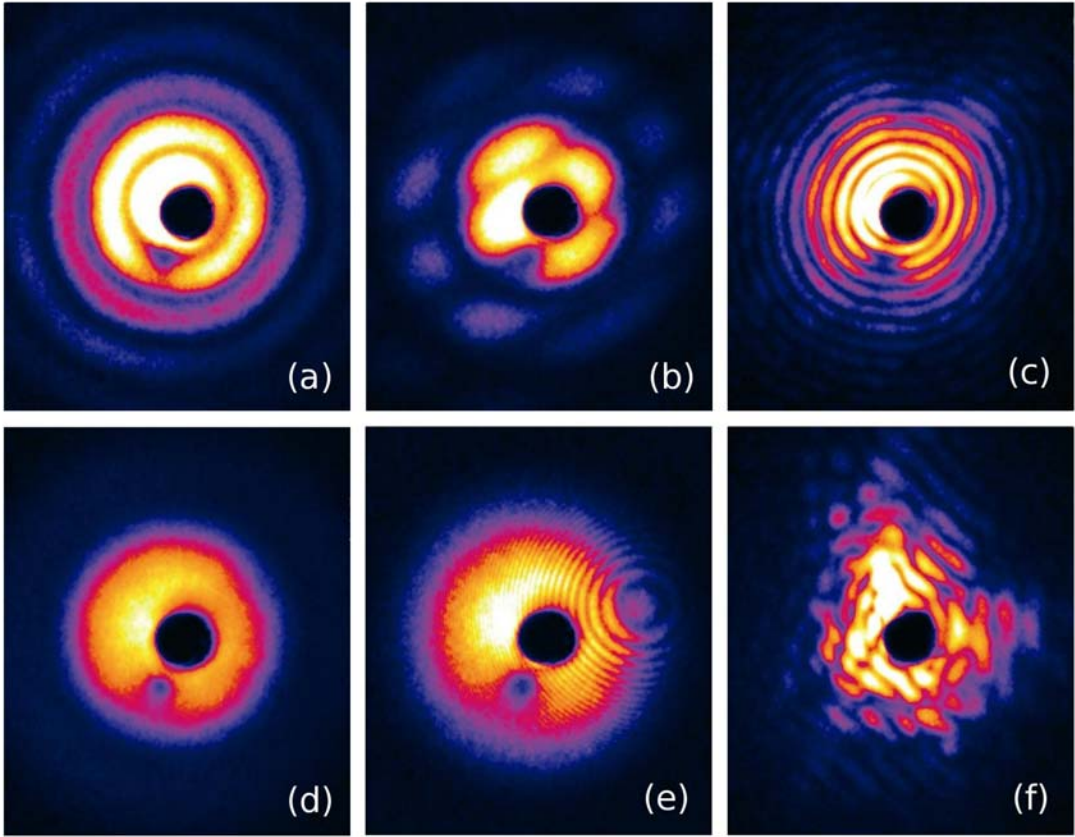


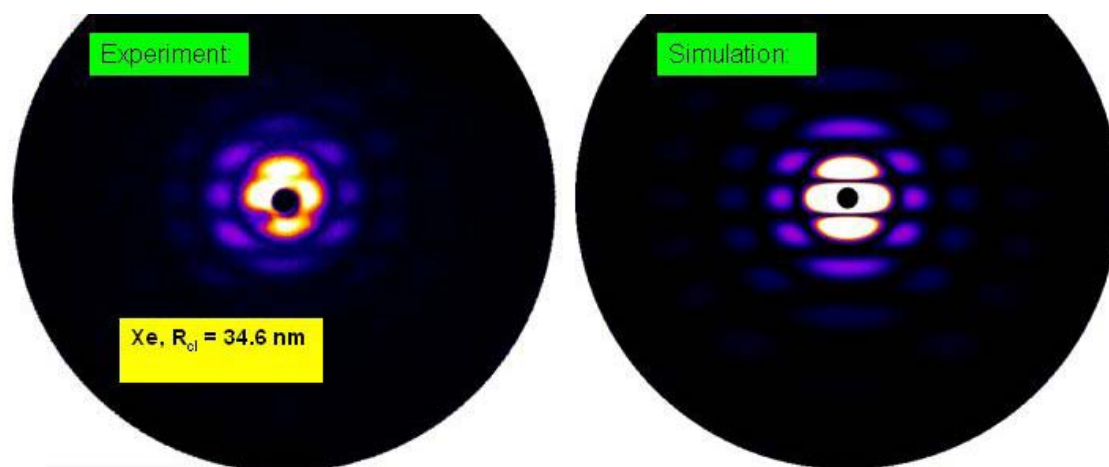


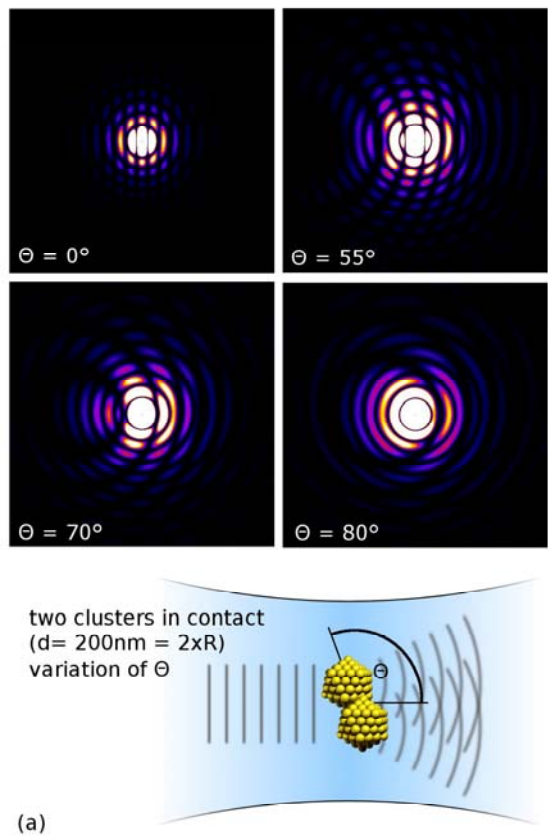












References

1. Ackermann, W. et al., *Operation of a free-electron laser from the extreme ultraviolet to the water window*. Nature Photonics, 2007. **1**: p. 336.
2. Bostedt, C., et al., *Experiments at FLASH*. Nuclear Instruments & Methods in Physics Research Section a-Accelerators Spectrometers Detectors and Associated Equipment, 2009. **601**(1-2): p. 108-122.
3. Wabnitz, H., et al., *Multiple ionization of atom clusters by intense soft X-rays from a free electron laser*. Nature, 2002. **420**: p. 482-485.
4. Ditmire, T., et al., *Interaction of intense pulses with atomic clusters*. Phys. Rev. A, 1996. **53**(5): p. 3379-3402.
5. Last, I. and J. Jortner, *Dynamics of the Coulomb explosion of large clusters in a strong laser field*. Phys. Rev. A, 2000. **62**: p. 13201-1-9.
6. Last, I. and J. Jortner, *Quasiresonance ionization of large multicharged clusters in a strong laser field*. Phys. Rev. A, 1999. **60**(3): p. 2215-2221.
7. Saalmann, U., C. Siedschlag, and J.M. Rost, *Mechanisms of cluster ionization in strong laser pulses*. J. Phys. B, 2006. **39**: p. R39-R97.
8. Krainov, V.P. and M.B. Smirnov, *Cluster beams in superintense femtosecond laser pulses*. Phys. Reports, 2002. **370**: p. 237-331.
9. Krainov, V.P., *Inverse stimulated bremsstrahlung of slow electrons under Coulomb scattering*. Journal of Physics B-Atomic Molecular and Optical Physics, 2000. **33**(8): p. 1585-1595.
10. Bostedt, C., et al., *Multistep ionization of argon clusters in intense femtosecond extreme ultraviolet pulses*. Physical Review Letters, 2008. **100**(13).
11. Hoener, M., et al., *Charge recombination in soft x-ray laser produced nanoplasmas*. Journal of Physics B-Atomic Molecular and Optical Physics, 2008. **41**(18).
12. Thomas, H., et al., *Shell explosion and core expansion of xenon clusters irradiated with intense femtosecond soft x-ray pulses*. Journal of Physics B-Atomic Molecular and Optical Physics, 2009. **42**(13).
13. Mitzner, R., et al., *Direct autocorrelation of soft-x-ray free-electron-laser pulses by time-resolved two-photon double ionization of He*. Physical Review A, 2009. **80**(2).
14. Tiedtke, K. and e. al., *The soft x-ray free-electron laser FLASH at DESY: beamlines, diagnostics and end-stations*. New Journal of Physics, 2009. **11**(2): p. 023029.
15. Buck, U. and R. Krohne, *Cluster size determination from diffractive He atom scattering*. J. Chem. Phys., 1996. **105**: p. 5408.
16. Karnbach, R., et al., *CLULU: An experimental setup for luminescence measurements on van der Waals clusters with synchrotron radiation*. Rev. Sci. Instr., 1993. **64**(10): p. 2838-2849.
17. Lengen, M., et al., *Site-specific excitation and decay processes in XeAr clusters*. Phys. Rev. Lett., 1992. **68**: p. 2362.
18. Laarmann, T., et al., *Tightly bound excitons in small argon clusters: Insights from size-dependent energy shifts*. Phys. Rev. B, 2002. **66**: p. 205407.
19. Danylchenko, O.G., et al., JETP Lett., 2006. **84**: p. 324.
20. Laarmann, T., et al., *Interaction of Argon Clusters with Intense VUV-Laser Radiation: The role of Electronic Structure in the Energy-Deposition process*. Phys. Rev. Lett., 2004. **92**: p. 143401.
21. Santra, R. and C. Green, *Xenon clusters in intense VUV Laser fields*. Phys. Rev. Lett., 2003. **91**: p. 233401.
22. Bauer, G., *Small rare gas clusters in laser fields: ionization and absorption at long and short laser wavelength*. J. Phys. B, 2004. **37**: p. 3085-3101.
23. Siedschlag, C. and J.M. Rost, *Small rare gas clusters in soft x-ray pulses*. Phys. Rev. Lett., 2004. **93**(4): p. 43402.

24. Jungreuthmayer, C., et al., *Intense VUV laser cluster interaction in the strong coupling regime*. Journal of Physics B-Atomic Molecular and Optical Physics, 2005. **38**(16): p. 3029-3036.
25. Ziaja, B., et al., *Energetics, Ionization, and Expansion Dynamics of Atomic Clusters Irradiated with Short Intense Vacuum-Ultraviolet Pulses*. Physical Review Letters, 2009. **102**(20).
26. Walters, Z.B., R. Santra, and C.H. Greene, *Interaction of intense vuv radiation with large xenon clusters*. Physical Review A, 2006. **74**(4): p. 043204.
27. Fukuzawa, H., et al., *Dead-time-free ion momentum spectroscopy of multiple ionization of Xe clusters irradiated by euv free-electron laser pulses*. Physical Review A, 2009. **79**(3).
28. Richter, M., et al., *Extreme Ultraviolet Laser Excites Atomic Giant Resonance*. Physical Review Letters, 2009. **102**(16): p. 163002.
29. Cooper, J.W., *Photoionization from Outer Atomic Subshells. A Model Study*. Physical Review, 1962. **128**(2): p. 681 LP - 693.
30. Hau-Riege, S.P., et al., *Encapsulation and Diffraction-Pattern-Correction Methods to Reduce the Effect of Damage in X-Ray Diffraction Imaging of Single Biological Molecules*. Physical Review Letters, 2007. **98**(19): p. 198302.
31. Rusek, M. and A. Orlowski, *Different mechanisms of cluster explosion within a unified smooth particle hydrodynamics Thomas-Fermi approach: Optical and short-wavelength regimes compared*. Physical Review A, 2005. **71**(4).
32. Ziaja, B., et al., *Femtosecond non-equilibrium dynamics of clusters irradiated with short intense VUV pulses*. New Journal of Physics, 2008. **10**.
33. Siegbahn, K., C. Nordling, G. Johannsson, J. Hedman, P.F. Heden, K. Hamrin, U. Gelius, T. Bergmark, L.O. Werme, R. Manne. Y. Baer,, *ESCA applied to free molecules*. 1969, Amsterdam: North-Holland.
34. Laarmann, T., et al., *Emission of Thermally activated Electrons from Rare Gas Clusters irradiated with intense VUV light from a Free Electron Laser*. Phys. Rev. Letters, 2005. **95**: p. 63402.
35. Ziaja, B., et al., *Emission of electrons from rare gas clusters after irradiation with intense VUV pulses of wavelength 100 nm and 32 nm*. New Journal of Physics, 2009. **11**.
36. Iwayama, H., et al., *Frustration of direct photoionization of Ar clusters in intense extreme ultraviolet pulses from a free electron laser*. Journal of Physics B-Atomic Molecular and Optical Physics, 2009. **42**(13).
37. Georgescu, I., U. Saalman, and J.M. Rost, *Clusters under strong vuv pulses: A quantum-classical hybrid description incorporating plasma effects*. Physical Review A, 2007. **76**(4): p. 043203.
38. Bostedt, C., et al., *Fast electrons from multi-electron dynamics in xenon clusters induced by inner-shell ionization*. New Journal of Physics, 2010. **in press**.
39. Neutze, R., et al., *Potential for biomolecular imaging with femtoscond X-ray pulses*. Nature, 2000. **406**: p. 752-757.
40. Chapman, H.N. and M.J.B. Anton Barty, Sébastien Boutet, Matthias Frank, Stefan P. Hau-Riege, Stefano Marchesini, Bruce W. Woods, Sas carona Bajt, W. Henry Benner, Richard A. London, Elke Plönjes, Marion Kuhlmann, Rolf Treusch, Stefan Düsterer, Thomas Tschentscher, Jochen R. Schneider, Eberhard Spiller, Thomas Möller, Christoph Bostedt, Matthias Hoener, David A. Shapiro, Keith O. Hodgson, David van der Spoel, Florian Burmeister, Magnus Bergh, Carl Caleman, Gösta Hultdt, M. Marvin Seibert, Filipe R. N. C. Maia, Richard W. Lee, Abraham Szöke, Nicusor Timneanu and Janos Hajdu, *Femtosecond diffractive imaging with a soft-X-ray free-electron laser*. Nature Physics, 2006. **2**: p. 839-843.
41. Bostedt, C., et al., *Ultrafast scattering as a probe for transient states of matter*. to be published, 2010.
42. Rupp , D., et al., to be published, 2010.
43. Born, M. and E. Wolf, *Principle of Optics*. 2002, Cambridge: Cambride University Press.
44. de Castro, A.R.B., et al., *Numerical simulation of small angle scattering (SAXS) for large atomic clusters*. Journal of Electron Spectroscopy and Related Phenomena, 2008. **166**: p. 21-27.

45. Rupp , D., *Simulation und Auswertung von Streuexperimenten am FEL für weiche Röntgenstrahlung*. 2008, TU-Berlin: Berlin.
46. Raines, K.S., et al., *Three-dimensional structure determination from a single view*. *Nature*. **463**(7278): p. 214-217.

Present address:

ⁱ Linac Coherent Light Source, SLAC National Accelerator Laboratory, 2575 Sand Hill Road, Menlo Park, CA 94025, USA

ⁱⁱ Department of Physics, Western Michigan Univeristy, Kalamazoo, Mi, 49008, USA

ⁱⁱⁱ Department of Physics, University of Texas at Austin, Austin, Tx 78712, USA